DETAILED MODELLING

OF

PHOTOVOLTAIC SYSTEM COMPONENTS

by

Jürgen Helmut Eckstein

A thesis submitted in partial fulfillment of the
requirements for the degree of

MASTER OF SCIENCE

(Mechanical Engineering)

at the

UNIVERSITY OF WISCONSIN - MADISON

1990

ABSTRACT

To predict the performance of photovoltaic powered energy systems, computer models of several system components have been developed. The computer models are integrated into TRNSYS, a simulation program developed by the Solar Energy Laboratory.

TRNSYS has been proven to be an accurate program in predicting and analyzing solar thermal and other energy systems. It has a modular structure and consists of a variety of individual subroutines which represent real physical devices. These components can be connected to systems and simulations can be run over different time periods.

This thesis describes the models of PV energy systems which have been developed. These are the photovoltaic arrays, a maximum power tracker, and different types of loads. Two different water pumping systems have been chosen. The first is a direct coupled system, consisting of a DC-motor and a centrifugal pump. In this case the motor is direct coupled to the PV array, i.e. there is no storage device included. The second system is a system with battery storage, where a charge controller is necessary to protect the battery for overcharging and deep discharge. In addition components

representing a resistive load and a ventilator type load are developed. Simulations of real systems are run to validate the models.

The implementation of the computer models into TRNSYS provides the possibility to run detailed simulations. Parameter studies can be done easily and thus an important tool for designing and predicting a PV system is obtained. The way the components are written and the structure of TRNSYS allows the user to add his or her own load components.

ACKNOWLEDGEMENTS

Special thanks go to my advisors Professor William A. Beckman and Professor John A. Duffie: for considering my interests in this research and making the project possible, for teaching me how to get down to a problem and for all their motivation and help.

I am very grateful to had the opportunity to complete my master degree here at the Solar Energy Laboratory. My time in the lab has been very intense and enjoyable. I have never experienced such a stimulating working environment before. I am going to miss working in the Lab, the seminars the discussions with students from all over the globe and especially all the great social events we had. Thank you, Sandy, John, Bill and Jack and all the students to make this laboratory not solely a place to work but a great place to be.

I would like to thank all those people who contributed to this thesis. Thanks to Jim Dunlop who provided me with experimental data and thanks to all people who supported me with information. Thanks to Ruth for helping me with computer and TRNSYS problems.

My stay in Madison was made possible by the German Academic Exchange Service (DAAD) and the Institut für Werkzeugmaschinen at the University of Stuttgart. I am

grateful to Dr. Lang and Thomas Utz for putting their personal effort in this program to keep it running and to make this great study abroad experience possible.

For telling me everything about football and basketball, I am thankful to my roommates. Their effort to get rid of my accent has unfortunately been less successful.

I want to thank my parents, and my brothers Wolfgang and Bernd for their financial and moral support and for all the letters and care packages. I am glad that you were able to visit me here in Madison and I am looking forward to see you all again soon.

Finally very special thanks to Ulrike for her steady and loving support. Thanks for being patient with me in this long distance relation and putting up with me through all this. Thanks for being you.

Solar Energy Laboratory

University of Wisconsin-Madison

TABLE OF CONTENTS

LIST OF FIGURES

Figure	Description	Page

LIST OF TABLES

NOMENCLATURE

Roman Symbols

A	- completion factor	
A	- cross sectional area	$[m^2]$
a	- fan constant	
AREA	- PV module area	$[m^2]$
b	- fan constant	
C	- friction coefficient	
c	- fan constant	
CP	- number of battery cells connected in parallel	
CS	- number of battery cells connected in series	
D	- diode diffusion factor	
D	- diameter	$[m]$
E_{SC}, E_{SD}	- open ciruit voltages (constant)	$[V]$
F	- objective function	
F	- fractional state of charge	
f	- friction factor	
Fail	- failure message	
FF	- fill factor	

Flag	- control signal	
g	- gravity constant	$[m/s^2]$
G_C, G_D	- small-valued coefficients of depth of discharge	
Guard	- control signal	
H	- head	$[m]$
H	- fractional depth of discharge	
hf	- head loss	$[m]$
I	- current	[amps]
I_A	- armature current	[amps]
I_C	- current corresponding to VC	[amps]
I_D	- diode current	[amps]
I_F	- field current	[amps]
I_L	- light current	[amps]
I_O	- reverse saturation current	[amps]
J	- Jacobian matrix	
K	- resistance coefficient	
k	- Boltzmann constant	$[J/K]$
k	- motor constant	
k_1, k_2	- constants	
k_f	- motor constant	
L	- length	$[m]$
L_A	- armature inductance	[henry]
L_F	- field inductance	[henry]
M_{AF}	- mutual inductance	[henry]
m_C, m_D	- battery cell type parameters	

Mode	- control signal	
n	- speed $= \dfrac{\omega}{2\pi}$	[1/s],[Rpm]
N	- speed	[1/s]
N	- ratio	
NCS	- number of cells connceted in series per module	
NP	- number of modules connected in parallel	
NS	- number of modules connected in series	
P	- power	[watts]
P_{ik}	- cofactor	
Q	- flow rate	[m³/s]
Q	- battery capacity (SOC)	[Ah]
q	- electron charge constant	[C]
Q_C, Q_D	- capacity parameters on charge, discharge	
Q_M	- rated capacity	[Ah]
R	- resistance	[ohms]
R_A	- armature resistance	[ohms]
R_F	- field resistance	[ohms]
R_S	- series resistance of the PV cell	[ohms]
$R_{SC,D}$	- internal resistance of battery on charge, discharge	[ohms]
Signal	- control signal	
SOC	- battery state of charge	[Ah]
SV	- control signal	
T	- torque	[Nm]
t	- time	
T_A	- ambient temperature	[°K]

T_C	- cell temperature	[°K]
U_L	- overall loss coefficient	
Util	- utilization of the PV array	
V	- voltage	[V]
$\overline{V}$	- average velocity	[m/s]
V_C	- cutoff voltage on charge	[V]
V_D	- cutoff voltage on discharge	[V]

Greek Symbols

γ	- shape factor	
ε_A	- electromotive force	[V]
ε_G	- material bandgap energy	[eV]
η	- efficiency	
μ_{ISC}	- temperature coefficient of short circuit current	[A/K]
μ_{VOC}	- temperature coefficient of open circuit voltage	[V/K]
ν	$-\dfrac{q}{k\, T_{C,REF}}$	[1/V]
ρ	- density	[kg/m^3]
Φ	- irradiance	[W/m^2],[kJ/m^2]
$\tau\alpha$	- transmittance absorptance product	
ϕ	- magnetic flux	[Wb]
ω	- angular velocity	[rad/s]

Additional Subscripts and Superscripts

absorbed	- absorbed
amb	- ambient
ave	- average
B	- battery
bh	- brake horsepower
C	- charge
CA	- charge again
D	- discharge
DA	- discharge again
DI	- diode
dissipated	- dissipated
elec	- electrical
electric	- electrical
fan	- fan
guess	- guess value
hyd	- hydraulic
load	- load
loss	- loss
LOW	- lower limit
M	- motor
MAX	- maximum
mech	- mechanical
MIN	- minimum
MP	- maximum power

new	- new
NOCT	- nominal operating cell temperature
nom	- nominal
OC	- open circuit
off	- shutoff condition
pump	- pump
PV	- photovoltaic
rated	- rated
REF	- reference condition
SC	- short circuit
shaft	- shaft
stat	- static
syst	- system
tol	- tolerance
tot	- total
visc	- viscous

_____ *Chapter 1* _____

INTRODUCTION

1.1 BACKGROUND

The origin of Photovoltaic (PV) energy conversion technology goes back in 1839, when Becquerel first discovered the PV effect. Photovoltaic energy conversion is the direct conversion of radiative energy, in form of sun-light, into electrical energy. Becquerel conducted experiments with acidic aqueous solutions and noble metal electrodes. The first work on solid state PV devices was done in 1876. The investigated material was selenium with an energy conversion efficiency which never exceeded more than approximately 2%. In 1954 the Bell Telephone Laboratories produced the first practical Solar Cell, a single crystal silicon type cell with an energy conversion efficiency up to 6%. Until the mid-1970s the development of the new energy technology has been rather moderate and has been determined by the dominant conventional energy technologies, the fossil fuels, especially coal,oil and natural gas. In addition the research emphasis was on the development of nuclear energy. In this time period PV power generation had only success in space applications.

During the last ten years the situation has been changed dramatically. Tremendous improvements have been attained in increasing the energy conversion efficiency,

reducing costs of cells, and different semiconductor materials have been investigated. The world record conversion efficiency for the most common solar cell, the single crystal silicon cell, was reported in 1988 with 22.8% efficiency, non-sunconcentrated and under laboratory conditions. The highest efficiency was obtained for a crystalline gallium arsenide (GaAs) cell with 31% efficiency at 350 suns (1988). More recent developments of Solar cells, the *thin film* cells consisting of polycrystalline copper indium diselenide (CuInSe), and amorphous silicon cells, showed both efficiencies of more than 14% [1]. New production technologies and automation reduced the selling price of PV cells and led to a growth of the PV industry. Some terrestrial PV systems mainly for remote applications are considered to be economical and utility interactive PV systems are predicted to become competitive in the 1990s.

Several factors are responsible for this evolution. The most significant factors are the world wide increase in energy demand and the fact that the fossil energy sources are finite and that they becoming more and more expensive. Another important issue is the impact of the energy technologies on the environment. Burning fossil fuels causes air pollution and is among other effects responsible for the so called *greenhouse effect*. Nuclear energy technology is afflicted with a possible danger and the storage problem of nuclear waste. In contrast to that, the advantage of the PV generated energy is apparent. It is a clean energy technology and is predicted to have a significant contribution to the world energy production towards the end of this century. This thesis introduces a tool for estimating the performance of PV power generation systems.

1.2 OBJECTIVE

One of the most important fields in PV technology is system design. Despite of the improvements in increasing the energy conversion efficiency, in practical applications the efficiencies are still relatively low and upper limits are set due to physical properties. Therefore a great value has to be set on designing the components of a PV system. A PV system works only properly if all the components connected to a PV array match to each other.

The task for this research is to develop computer models which are capable to simulate real PV system components accurately. The detailed models are integrated in the *Transient System Simulation Program* (TRNSYS) developed at the University of Wisconsin-Madison [2]. This provides a tool to predict and analyze the performance of PV powered energy systems and thus to improve system design.

TRNSYS has been proven to be an accurate program in simulating solar thermal and other energy systems. It is designed to simulate transient systems, it provides important means of outputting results and means of handling meteorological data input. Fixed collector surface as well as single-axis and two-axis tracking simulations are possible. It has a tremendous flexibility, i.e. simulating different system configurations is easily possible. Therefore it is an ideal frame for the implementation of PV system components. *TRNSYS* is described more detailed in section 1.3.

Figure 1.1 shows typical PV system configurations. Systems are distinguished considering several factors. The basic distinction is whether the load requires DC or

AC power (dashed line in Figure 1.1). Systems with AC loads require a DC-AC inverter. Another distinction is whether it is a so called stand alone system or a utility integrated system. Stand alone systems are not connected to the grid but may have other backup sources like a diesel generator. Applications are installed in remote locations, especially in developing countries. Utility integrated systems may deliver energy to the grid and draw energy from it when necessary.

DC loads
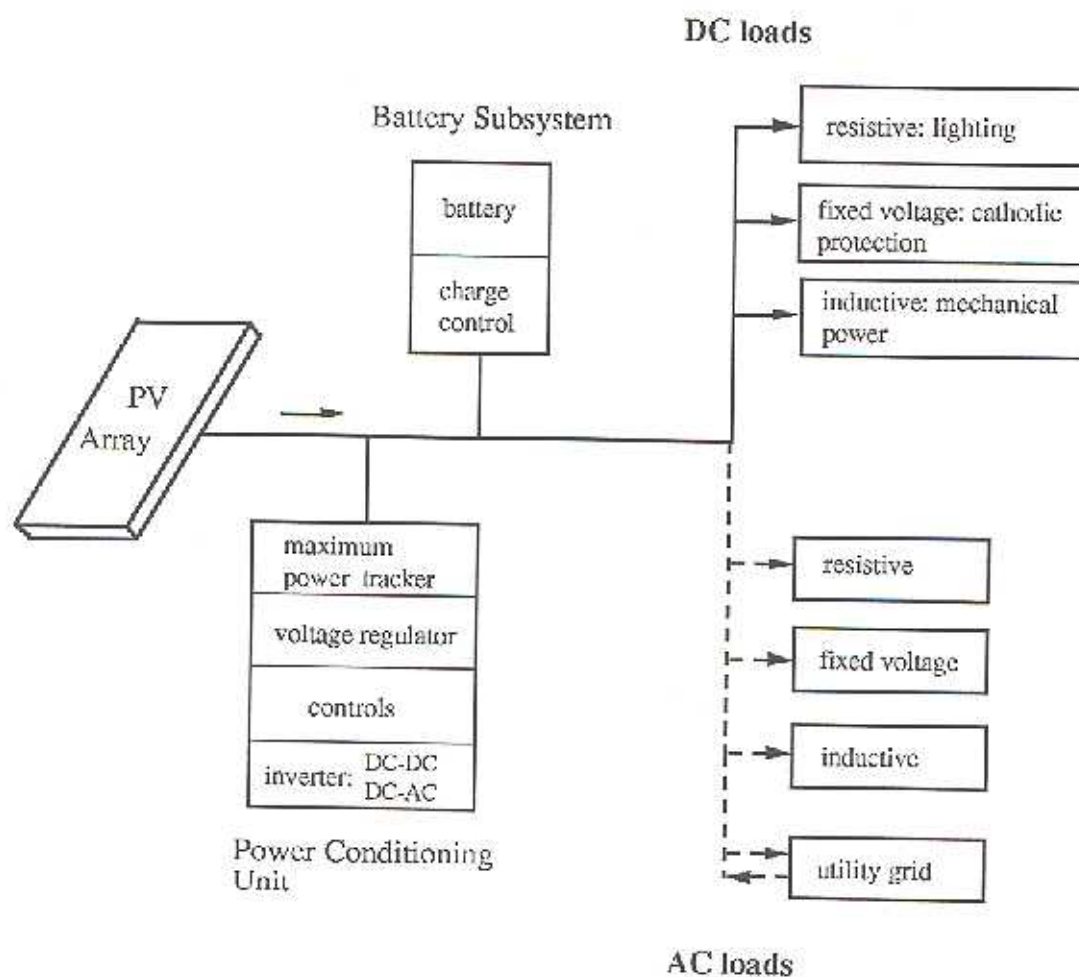
Figure 1.1 PV system configuration

Stand alone systems may have a battery subsystem for energy storage. Systems where the load component is directly connected to the PV array, without any power conditioning device or battery subsystem, are called direct coupled systems. Common applications are water pumping systems. Systems with battery storage require charge control to protect the battery from overcharging and deep discharge.

Maximum power tracker are used to optimize the performance of a PV array, i.e. to produce the largest power output of a PV cell which leads to a reduction in PV array area. Some loads, such as fixed voltage loads, require voltage regulation. Maximum power tracker, voltage regulators, controller and inverter are combined into the power conditioning unit.

Several computer based models exist for simulating and estimating the performance of PV systems. A review of available computer models was done by Smith and Reiter [4] in 1984. Table 1 shows a brief summary of this review done by Townsend [3].

In this research, models of the basic components of a PV stand alone system are developed. These are the PV array, a maximum power tracker and a battery storage subsystem. Two standard battery charge controllers, a series and a shunt type controller, are developed. As load examples, an ohmic resistor, a ventilator type load and water pumping load are chosen. Models of a series and a separately excited permanent magnet DC-motor, and models of a centrifugal pump and a fan are developed.

MODEL	ORIGINATOR	ATTRIBUTES
Townsend M.S. Thesis	UW-Madison	Simplified; Direct-coupled or Maximum Power-Tracked systems; no storage or economics; for fixed flat plate (f.p.) collectors.
PV f-Chart	f-Chart Software	Simplified; only for Maximum Power-Tracked (MPT) systems; includes storage and economics; for fixed or tracking, f.p. or concentrating (con.) collectors.
PVFORM	Sandia Labs	Detailed, but can skip days to speed calcs.; MPT systems only; incl. storage and economics; for fixed, tracking f.p.
PVPM (PV Performance Model)	Electric Power Research Inst.	Detailed; MPT systems only; no storage or economics; fixed, tracking f.p. or con.
E&R (Engr. & Reliability)	Jet Prop. Lab	Detailed; MPT or fixed voltage operation; no storage or econ.; fixed, tracking f.p.
LCP (Lifetime Cost & Perf.)	Jet Prop. Lab	Detailed; MPT only; no storage; includes economics; fixed, tracking f.p.
SOLCEL-II (Solar Cell Model, Version 2)	Sandia Labs	Detailed w/day skip option; MPT, fixed, or battery-coupled voltage sys.; incl. stor. and econ.; fixed, tracking f.p. or con.
SOLSYS (Solar Energy System Analysis Prog.)	Sandia Labs	Detailed; MPT, fixed voltage, battery-coupled, or load $I=f(V^2)$ operation; incl. storage; no econ.; fixed or tracking f.p. or con.
TRNSYS/ASU	UW-Mad/Arizona State/Sandia	Detailed; MPT, batt.-coupled sys.; incl. storage and econ.; fixed, tracking f.p. or con.
TRNSYS/MIT	UW-Mad/Mass. Inst. of Tech.	Detailed; MPT, fixed voltage operation; no storage, econ.; fixed or tracking f.p.
PV-TAP	BDM/Sandia	Transient, not appl. to long-term est.
Stand-Alone Model	Sunrise Assoc/ Cleveland St.	Simplified; fixed voltage only; includes storage and econ.; fixed f.p. only.

Table 1.1 PV Performance Model Summary. From Townsend [3].

The thesis is organized in the following way: First the developed models are presented. Chapter 2 discusses the model of a PV array and its electrical behavior. The load components are treated in Chapter three. The components of a battery subsystem, i.e. the battery itself and the charge controllers, and a model of a maximum power tracker are discussed in Chapter four. Chapter five is an analysis of the investigated PV systems. Simulations and comparisons to experimental data are discussed in Chapter six. Finally, conclusions and recommendations for future work are presented in Chapter seven.

1.3 THE SIMULATION PROGRAM

TRNSYS has a modular structure. It contains a variety of individual subroutines, the components, representing the mathematical model description of real physical devices. The modular nature of *TRNSYS* facilitates modeling number of different system configurations.

A system is defined to be a set of components interconnected in such a manner as the components of a real system would be connected to each other. A *TRNSYS* system contains, in addition to a real system, components which make meteorological data useful for simulations and facilities to output results. The means to construct such a system is called the *TRNSYS* deck. It is a computer file containing all the necessary components and information to run a simulation.

A component is identified by its mathematical description and by information

explaining the interface to its environment, i.e. to other components and to the user. This information is the parameters, inputs and outputs of a component. The inputs and parameters are required to perform the calculations which produce the outputs. In a system, the outputs of one component may be the inputs of another component. The parameters and the interconnection information determining the data flux among the components have to be specified in the *TRNSYS* deck.

The simulation must be driven by forcing functions, such as load profiles or meteorological data. For a PV system the forcing functions are the solar radiation and the temperature data, usually given on an hourly basis. For many locations data are available for an average year, known as *typical meteorological year* (TMY) data. TMY data provide the solar radiation on a horizontal surface and the temperatures. In general any user supplied meteorological data can be made available to *TRNSYS* simulations. A component, called the solar radiation processor, converts the solar radiation data from the values on a horizontal surface to any tilted surface, with or without tracking.

For any timestep specified by the user, *TRNSYS* will solve all the equations defining the system via an iterative process, called successive substitution. During the calculations within a timestep, all the time dependent variables are considered to be constant. The solar radiation processor interpolates data for chosen timesteps smaller than the timesteps for which data are available.

The user has to specify the length of a timestep and the length of the simulation period, which can be of any length, in the deck. A convergence tolerance for the process of successive substitution has to be set also by the user. The description of components and system modelling procedures in the following chapters should gradually familiarize the reader with the specific features of *TRNSYS*.

MODEL FOR A
PHOTOVOLTAIC CELL

In this chapter a mathematical model describing the current-voltage behavior of a PV cell is developed. Techniques to obtain the parameters and a solution of the relationship are presented. The sensitivity of environmental influences, such as irradiance and temperature on the model, are examined and a *TRNSYS* component is formulated.

Many models of varying complexity describing the behavior of a PV cell exist. To choose an appropriate model for detailed simulation, several factors need to be considered.

The most important one is the accuracy which can be obtained. There is always a tradeoff between accuracy and simplicity. To minimize the computational effort which is involved in long-term performance prediction, the model should be kept as simple as possible without sacrificing the required accuracy.

In contrast to the utility grid, a PV cell is not a fixed voltage source. Detailed simulation requires that the model is able to predict current and voltage over the entire operating voltage range. Some simplified models provide current-voltage behavior just at maximum power, open voltage and short circuit current points.

9

Another factor is whether the data needed to drive the model is available, i.e. can the data be obtained in the relevant literature and/or manufacturers publications. Sophisticated models often require data which is generally not available.

Townsend [3] analyzed several models which satisfy the criteria stated above. He proposed a four parameter model to be the most appropriate one for long-term performance estimation. This model provided the best match with experimental data, required reasonable computational effort, and the information needed to obtain the four parameters is readily available from manufacturers brochures. For these reasons it has been selected for the use in *TRNSYS* and will be described in the following sections.

2.1 A PV EQUIVALENT ELECTRICAL CIRCUIT

The electrical behavior of the chosen model is described by the equivalent circuit shown in Figure 2.1. It is capable of modelling a flat-plate non-sunconcentrated collector and it is useful for steady state calculations only. Long-term performance prediction does not require consideration of the transient behavior of a PV cell.

The light current, I_L, represents the current generated from the incident sunlight on the cell and it is generally proportional to solar irradiance. The diode characterizes the semiconductor junction of the cell material. Thus the diode current, I_D, is the current flowing internally across the cell's semiconductor junction. All the internal dissipative electrical losses are lumped together into the series resistance, R_S. The cell resistance elements are the semiconductor material itself and the contact interfaces.
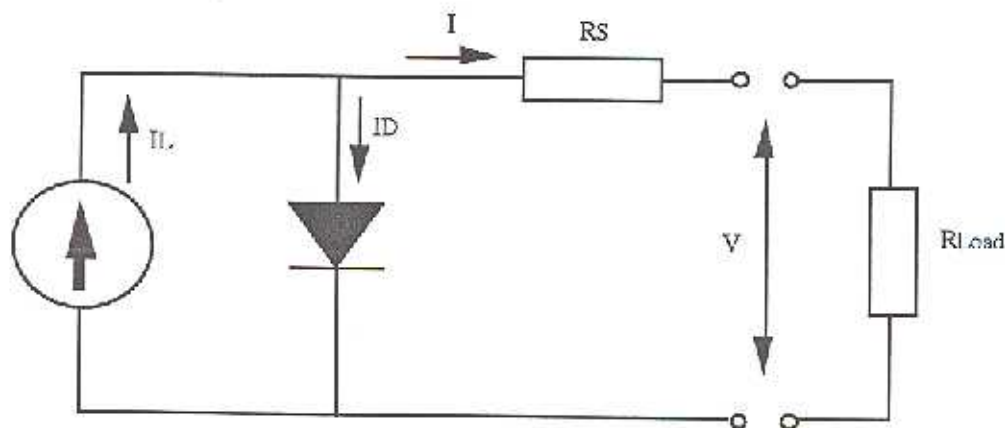
Figure 2.1 PV cell equivalent circuit

Some models also include a shunt resistance in parallel with the diode to account for leakage losses. A part of the generated energy is lost through internal cell leakage caused by a recombination current in the pn-junction and the outer edges of the cell [5]. Shunt resistance effects the I-V curve shape significantly only at very low radiation levels and even then only at high voltages. A comparison of the effect of shunt resistance on modeled I-V behavior has been conducted by Townsend [3]. The shunt resistance is of a much higher order than the series resistance. Even for an unrealistically low shunt resistance the effect on the generated power was negligible. This led to the assumption made in this model that the shunt resistance is infinite and, therefore, it can be neglected.

The light current and the diode current define the cell I-V shape as shown in Figure 2.2. The non-illuminated cell has the same I-V characteristics as a diode. When the cell is being illuminated, the light current is added to the diode current. The only difference between a diode and the cell pn-junction is that the diode consumes energy

while the cell produces energy. The curves in Figure 2.2 are drawn with the current sign convention in Figure 2.1.
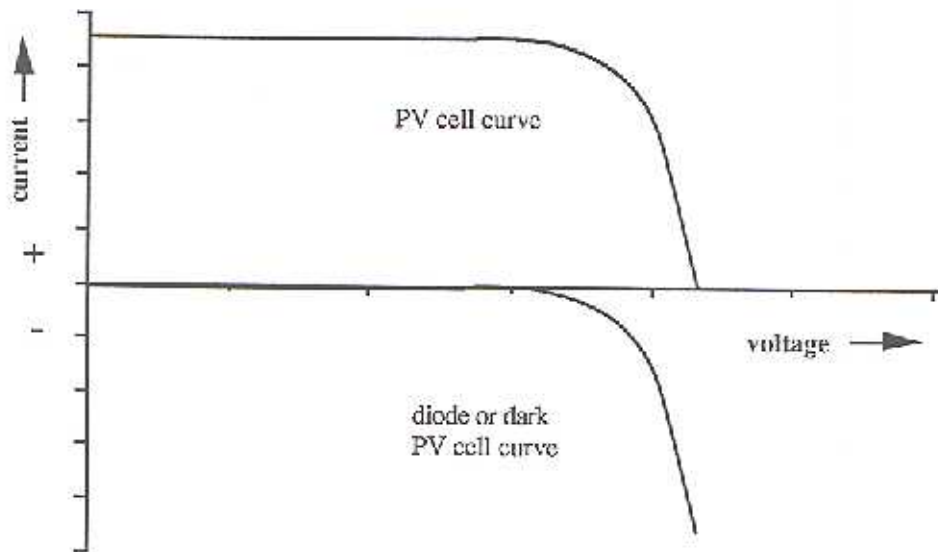
Figure 2.2 Cell and diode I-V curves for ideal PV cell

Applying Kirchoff's law of current, the terminal current of the cell is

$$I = I_L - I_D \tag{2.1.1}$$

The light current is related to irradiance and temperature and the light current measured at some reference condition:

$$I_L = \left(\frac{\Phi}{\Phi_{REF}}\right)(I_{L,REF} + \mu_{ISC}(T_C - T_{C,REF})) \tag{2.1.2}$$

where

$I_{L,REF}$ = light current at reference condition [amps]

Φ, Φ_{REF} = irradiance, actual and at reference condition [W/m2]

$T_C, T_{C,REF}$ = cell temperature, actual and at reference condition [degree Kelvin]

μ_{ISC} = manufacturer supplied temperature coefficient of short circuit current
[amps/degree]

The diode current is given by the Shockley equation:

$$I_D = I_O \left(\exp\left(\frac{q(V+IR_S)}{\gamma k T_c} \right) - 1 \right) \qquad (2.1.3)$$

where

V = terminal voltage [volts]

I_O = reverse saturation current [amps]

γ = shape factor

R_S = series resistance [ohm]

q = electron charge constant, 1.602×10^{-19} C

k = Boltzmann constant, 1.381×10^{-23} J/K

The reverse saturation current is

$$I_O = D (T_C)^3 \exp\left(\frac{-q \varepsilon_a}{A k T_c} \right) \qquad (2.1.4)$$

where

D = diode diffusion factor

ε_G = material bandgap energy (1.12 eV for Si, 1.35 eV for GaAs)

A = completion factor

The reverse saturation current is actually computed by taking the ratio of equation (2.1.4) at two different temperatures, thereby eliminating D. Similar to the determination of I_L (equation 2.1.2), I_O is related to the temperature and the saturation current estimated at some reference condition:

$$I_O = I_{O,REF}\left(\frac{T_C}{T_{C,REF}}\right)^3 \exp\left[\left(\frac{q\,\varepsilon_G}{k\,A}\right)\left(\frac{1}{T_{C,REF}} - \frac{1}{T_C}\right)\right] \tag{2.1.5}$$

and thus the I-V characteristic is described by

$$I = I_L - I_O\left(\exp\left(\frac{q(V + IR_s)}{\gamma k T_c}\right) - 1\right) \tag{2.1.6}$$

The shape factor γ is a measure of cell imperfection and is related to the completion factor as $\gamma = A \times NCS \times NS$. NCS is the number of cells connected in series per module. A module is defined as an array of cells, usually encapsulated for protection, as it is supplied by manufacturer, and NS is the number of modules connected in series of the entire array.

The four unknown parameters are I_L, I_O, γ and R_S or more precisely the parameters at reference condition. While γ and R_S are assumed to be constant, I_L is a function of

irradiance and cell temperature and I_O is a function of temperature only. The evaluation of these parameters is presented in section 2.2. The cell temperature can be determined from the ambient temperature and with the help of some standard test information as will be shown in section 2.3.

For a given irradiance, cell temperature, and cell parameters, a continuous relationship of current as a function of voltage is given by equation (2.1.6). It is a nonlinear implicit equation and has to be solved numerically. The typical current-voltage and power-voltage output described by this equation is shown in Figure 2.3.
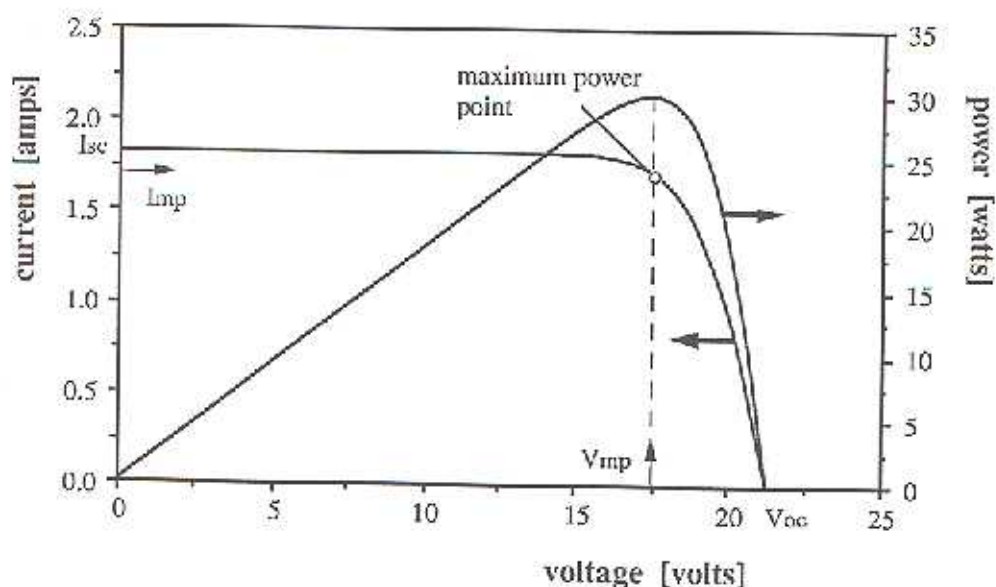
Figure 2.3 Current-voltage and power-voltage characteristics for a Solarex MSX-30 module, at 1000 W/m^2 and cell temperature = 25°C.

Looking at the I-V curve, the PV cell is a constant current source at low voltages with a current approximately equal to the short circuit current (I_{SC}). With increasing voltage at a certain point the current begins to drop off exponentially to zero at open

circuit voltage (V_{OC}). Over the entire voltage range, there is one point where the cell operates at the highest efficiency, this is the maximum power point. The goal of system design is to operate the cell at that point. System design, however, is complicated by the fact that the maximum power point varies with irradiance and temperature.

A basic factor which describes the quality of the I-V curve is the fill factor (FF):

$$FF = \frac{V_{MP} \, I_{MP}}{V_{OC} \, I_{SC}} \qquad\qquad (2.1.7)$$

V_{MP} and I_{MP} are the voltage and current corresponding to the maximum power point. The fill factor is used to rate the *squareness* of the I-V curve. The *squarer* the curve the larger the fill factor the greater is the maximum power output. The fill factor is used to compare different solar cells under the same reference conditions.

2.2 SOLUTION OF THE I-V EQUATION

As mentioned in section 2.1, the I-V equation (2.1.6) can be solved numerically for a given irradiance, cell temperature and a set of parameters (I_L, I_O, γ, R_S). The method used is *Newton's* method. The information needed to solve for these parameters is shown in Table 2.1. The bandgap energy is published in scientific literature. Everything else is supplied from manufacturer.

Symbol	Units	Name	From mfg?
Φ_{REF}	W/m²	plane of array irradiance, reference	Yes
Φ	W/m²	plane of array irradiance	No
$T_{C,REF}$	K	cell temperature, reference	Yes
T_C	K	cell temperature	No
$I_{SC,REF}$	A	short circuit current, reference	Yes
$V_{OC,REF}$	V	open circuit voltage, reference	Yes
$I_{MP,REF}$	A	maximum power point current, reference	Yes
$V_{MP,REF}$	V	maximum power point voltage, reference	Yes
NCS	1/system	number of cells in series within the system	Yes
μ_{ISC}	A/K	temperature coefficient of short circuit current	Yes
μ_{VOC}	V/K	temperature coefficient of open circuit voltage	Yes
ε_G	V	bandgap energy - semiconductor material property, assumed constant over flat plate PV operating temperatures; published in many texts	No
R_s	Ω	apparent (lumped) series resistance - if not provided by manufacturer, can be estimated by other methods	Some
Area	m²	net module area	Yes
$T_{A,NOCT}$	K	ambient temperature at Nominal Operating Cell Temperature (NOCT) test conditions	Yes
Φ_{NOCT}	W/m²	plane of array irradiance at NOCT conditions	Yes
$T_{C,NOCT}$	K	cell temperature at NOCT conditions	Yes

Table 2.1 Information required to solve for the model. From Townsend [3].

An obvious procedure to estimate the four parameters would be to find four independent relationships involving I_L, I_O, γ and R_S. A simultaneous solution could be obtained by solving this system of equations. This has been done by Townsend [3]. Because of the nonlinear nature of the system of equations, *Newton's* method or an equivalent method has to be used to solve the system. The solution of *Newton's* method is very sensitive to the initial guesses. Initial guesses far off the correct values may result in unrealistic or no solutions. Therefore, Townsend developed an alternate method. First he derived a method to estimate the series resistance parameter. This reduces the four unknown parameters to three. Solving for the remaining parameters is then possible at some reference condition, where the necessary data are available, using explicit relationships as discussed in section 2.2.1. The method to evaluate R_S is provided in section 2.2.2. The methods to evaluate these parameters in sections 2.2.1 and 2.2.2 are based on data for a single module. The method to scale up the parameters for the entire array is shown in section 2.2.3. Once I_L and I_O are known at reference condition, they can be updated for other conditions using equations (2.1.2) and (2.1.5). R and γ are assumed to be independent of temperature and irradiance and need not to be updated.

2.2.1 Evaluation of the Parameters

Information from the manufacturer is generally available at three points on the I-V curve: the voltage at open circuit $V_{OC,REF}$, the current at short circuit $I_{SC,REF}$, and the current and voltage at maximum power $I_{MP,REF}$ and $V_{MP,REF}$. The procedure to solve for the three parameters $I_{L,REF}$, $I_{O,REF}$ and γ_{REF} is by forcing the I-V curve through the

three given points. This is done by setting up a system of three equations. As it will be shown, this system can be simplified and an explicit solution is possible. The relationships for the given points are

at short circuit: $I=I_{SC}$ $V=0$

at open circuit: $I=0$ $V=V_{OC}$

at maximum power: $I=I_{MP}$ $V=V_{MP}$

Substituting these expressions successively in equation (2.1.6) and introducing an auxiliary variable ,v, to combine often repeated constants:

$$v = \frac{q}{k \, T_{C,REF}} \qquad (2.2.1)$$

The system of three equations is given by

$$I_{SC,REF} = I_{L,REF} - I_{O,REF} \left(\exp\left(\frac{v \, I_{SC,REF} \, R_s}{\gamma} \right) - 1 \right) \qquad (2.2.2)$$

$$0 = I_{L,REF} - I_{O,REF} \left(\exp\left(\frac{v \, V_{OC,REF}}{\gamma} \right) - 1 \right) \qquad (2.2.3)$$

$$I_{MP,REF} = I_{L,REF} - I_{O,REF} \left(\exp\left(\frac{v \, (V_{MP,REF} + I_{MP,REF} \, R_{s,REF})}{\gamma} \right) - 1 \right) \qquad (2.2.4)$$

Looking at Figure 2.1, at short circuit the series resistance causes a small voltage drop and hence a small part of the light current gets shunted through the diode instead of through the terminal. The order of the series resistance is so small that the fraction of

the light current shunted through the diode is about one millionth [3]. For practical use it can be assumed that the light current and the short circuit current are equal under all conditions. The product of $I_{O,REF}$ and the following term in parentheses of equation (2.2.2) can be omitted and a trivial solution for parameter $I_{L,REF}$ is obtained: $I_{L,REF}$ is equal to $I_{SC,REF}$.

Another simplification can be made regarding the -1 term in equations (2.2.3) and (2.2.4). In both cases, regardless of the size of the system, the exponential term is much greater than the -1 term. For this reason the -1 term can be neglected and the system of equations becomes

$$I_{L,REF} \approx I_{SC,REF} \tag{2.2.5}$$

$$0 \approx I_{SC,REF} - I_{O,REF} \exp\left(\frac{v \, V_{OC,REF}}{\gamma}\right) \tag{2.2.6}$$

$$I_{MP,REF} \approx I_{SC,REF} - I_{O,REF} \exp\left(\frac{v \, (V_{MP,REF} + I_{MP,REF} \, R_S)}{\gamma}\right) \tag{2.2.7}$$

Substituting equation (2.2.6) into equation (2.2.7) and solving for γ gives

$$\gamma = \frac{v \, (V_{MP,REF} + I_{MP,REF} \, R_S - V_{OC,REF})}{\ln\left(1 - \frac{I_{MP,REF}}{I_{SC,REF}}\right)} \tag{2.2.8}$$

Finally $I_{O,REF}$ is determined substituting γ into equation (2.2.6):

$$I_{O,REF} = I_{SC,REF} \exp\left(\frac{-v \, V_{OC,REF}}{\gamma}\right) \tag{2.2.9}$$

Each of these parameters is evaluated at the reference (i.e. known) condition for a PV module as supplied by the manufacturer. For other conditions, I_L may be updated using equation (2.1.2), and I_O may be recalculated using equation (2.1.5).

2.2.2 Evaluation of the Series Resistance

Several different methods have been developed to determine the series resistance. The method used in this study was proposed by Townsend [3]. Among the four methods he investigated, a method based on an iterative search for a proper value of R_S produced the best results. The method makes use of the temperature coefficient of the open circuit voltage, μ_{VOC}, which is often supplied by the manufacturer.

The basic idea behind the procedure is to derive an analytical expression for μ_{VOC}, using the equations presented in the previous section. As discussed in section 2.2.1, guessing a series resistance fixes the remaining parameters, I_O, γ and I_L (actually I_L is independent on R_S by equation (2.2.5). The estimated parameters are used to develop an analytical expression for μ_{VOC}. The reported and the analytical value for μ_{VOC} are compared and a binomial search routine, the *bisection method*, is used to converge on the proper value of μ_{VOC} by making new guesses for R_S.

The *bisection method* requires a lower and an upper limit for the convergence variable, in this case for R_S. The lower limit is chosen to be zero ohms. The resulting parameters are obtained using equations (2.2.5), (2.2.8) and (2.2.9):

$$I_{L,LOW} = I_{SC,REF} \tag{2.2.10}$$

$$\gamma_{LOW} = \frac{\nu \left(V_{MP,REF} - V_{OC,REF}\right)}{\ln\left(1 - \dfrac{I_{MP,REF}}{I_{SC,REF}}\right)} \tag{2.2.11}$$

$$I_{O,LOW} = I_{SC,REF} \exp\left(\frac{-\nu\, V_{OC,REF}}{\gamma_{LOW}}\right) \tag{2.2.12}$$

The upper limit for R_S is established by physical limitations. Three points on the I-V curve are fixed independent of the values of the parameters, that is, the open circuit, the short circuit and the maximum power point. The shape of the curve is described by the parameters, mainly by the shape factor γ. Since R_S fixes the remaining parameters, different values for R_S will effect the shape of the curve. It is observed that progressively higher values of R_S result in progressively lower values of γ. Thus the lowest value of γ would determine the upper limit for R_S. The low limit on γ is given by the number of cells in series, NCS, since γ is the product of the completion factor, A, and NCS, and A has a low limit of 1.0. The low limit of A corresponds to an ideal cell behavior, i.e. that each photon-generated electron-hole pair contributes to the cell current rather than recombining. Substituting γ equal to NCS, equation (2.2.8) may be rearranged to obtain the upper limit for R_S:

$$R_{S,MAX} = \frac{1}{I_{MP,REF}}\left[\frac{NCS}{\nu}\ln\left(1 - \frac{I_{MP,REF}}{I_{SC,REF}}\right) + V_{OC,REF} - V_{MP,REF}\right] \tag{2.2.13}$$

The upper limit for I_L is the same as the lower limit, because I_L is not affected by R_S, and I_O is recalculated according equation (2.2.9).

The analytical expression for μ_{VOC} is obtained by rearranging equation (2.2.6) to yield

$$V_{OC,REF} = \frac{\gamma}{\nu} \ln\left(\frac{I_{SC,REF}}{I_{O,REF}}\right) \tag{2.2.14}$$

and differentiating this expression with respect to cell temperature results in

$$\mu_{VOC} = \frac{\partial V_{OC,REF}}{\partial T_{C,REF}} = \frac{\gamma k}{q} \left[\ln\left(\frac{I_{SC,REF}}{I_{O,REF}}\right) + \frac{T_{C,REF}\,\mu_{ISC}}{I_{SC,REF}} - \left(3 + \frac{q\,\varepsilon_G}{A\,k\,T_{C,REF}}\right) \right] \tag{2.2.15}$$

This analytical value is compared to the measured value for μ_{VOC} and new guesses for R_S are made until the analytical and the empirical value match sufficiently.

2.2.3   Effect of Series/Parallel Groupings

The power output from single PV cells is relatively small (approximately 0.5 Watts). To produce the required voltage and power, PV cells are connected in series and parallel. PV cells are grouped into modules, the smallest assembly designed to produce dc-power and as mentioned before, the smallest unit available from manufacturer. Modules are combined into panels and those panels are connected together to build up the entire PV array. This way almost any desired I-V characteristic can be generated.

The parameters evaluated in section 2.2.1 and 2.2.2 are based on data input for a single module at some reference condition. To describe the I-V characteristic for the

entire array the parameters need to be scaled up in the following way:

$$I_{L,tot} = NP \times I_L \qquad (2.2.16)$$

$$I_{O,tot} = NP \times I_O \qquad (2.2.17)$$

$$\gamma_{tot} = NS \times \gamma \qquad (2.2.18)$$

$$R_{S,tot} = \frac{NS}{NP} \times R_S \qquad (2.2.19)$$

where NP is the number of modules connected in parallel and NS is the number of modules connected in series. This scaling method assumes that all modules in the array are alike. It is not possible to produce identical modules. In reality there will always be a difference between the overall value and the scaled values of the parameters. For production tolerances of $\pm$ 5-10 % however, the mismatch losses are not significant [6].

The effect of series and parallel groupings on the I-V characteristics is shown in Figure 2.4. Connecting cells in series will increase the voltage output, and connecting cells in parallel will increase the current output, corresponding to the expressions:

$$I_{tot} = NP \times I \qquad (2.2.20)$$

$$V_{tot} = NS \times V \qquad (2.2.21)$$
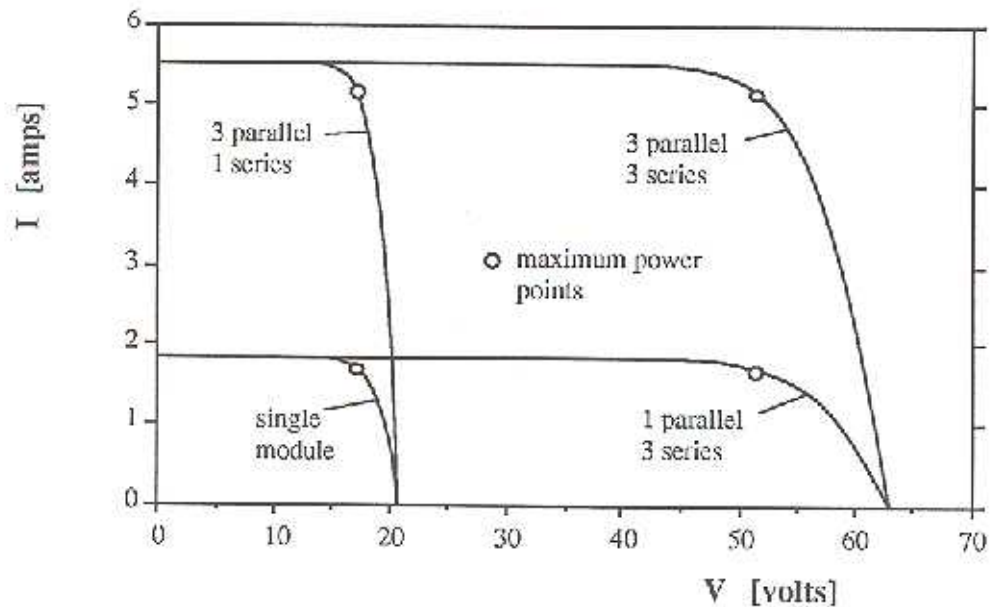
Figure 2.4 Effects of series and parallel connections of PV modules on I-V characteristics. Solarex MSX-30 module; 1000 W/m^2 and Tcell = 30°C

2.3 DETERMINING CELL TEMPERATURE

The cell temperature or more precisely the pn-junction temperature has a strong effect on the performance of a PV cell as will be shown later. The degree of accuracy, with which the cell temperature can be estimated, will effect the simulation results significantly. The method presented here is based on data obtained from a standard test called *Nominal Operating Cell Temperature* (NOCT) test. This information is available from manufacturer.

The cell temperature depends on the ambient temperature and to the rates at which incident energy is being absorbed, dissipated and converted to electricity. An energy (power) balance of the cell at steady state gives

$$P_{electric} = P_{absorbed} - P_{dissipated} \qquad (2.3.1)$$

where the single power terms are determined as follows:

The generated dc power:

$$P_{electric} = \Phi \; Area \; \eta \qquad (2.3.2)$$

η is the electric conversion efficiency.

The absorbed power (i.e. the absorbed solar energy) is

$$P_{absorbed} = \Phi \; Area \; \tau \; \alpha_{ave} \qquad (2.3.3)$$

$\tau \; \alpha_{ave}$ is an average transmittance-absorptance product, or the ratio of absorbed to incident energy, and is assumed to be constant with no correction for dependence on incidence angle.

The dissipated power (i.e. the thermal loss) is given by

$$P_{dissipated} = U_L \; Area \; (T_C - T_{amb}) \qquad (2.3.4)$$

U_L is an overall loss coefficient including convective and radiative heat losses from the cell top and bottom, and conduction through any mounting framework that may be

present. Conductive heat transfer within the cell is neglected in this analysis, because the cells are thin and have a small heat capacity. Hence the cell temperature is assumed to be the same within the entire cell.

Substituting equations (2.3.2) - (2.3.4) into equation (2.3.1) and then rearranging, an expression for the cell temperature is obtained:

$$T_C = T_{amb} + \frac{\Phi \, \tau \, \alpha_{ave}}{U_L} \left(1 - \frac{\eta}{\tau \, \alpha_{ave}}\right) \qquad (2.3.5)$$

The cell electric conversion efficiency η varies from zero at short circuit and open circuit points to the maximum efficiency, depending on the actual cell operating point. To ascribe η a constant value somewhat in the range of 0-20% does not affect the cell temperature calculation significantly. The difference in calculated cell temperature, at a typical average irradiance of about 600 W/m^2, between 5% and 20% efficiency is approximately 3°C for a assumed $\tau \, \alpha_{ave}$ of 0.9. This is in the range of uncertainty inherent in cell temperature measurements even for slightly different values for $\tau \, \alpha_{ave}$. The chosen value for η is the maximum power point efficiency at the given reference condition:

$$\eta_{REF} = \frac{I_{MP,REF} \, V_{MP,REF}}{\Phi_{REF} \, Area} \qquad (2.3.6)$$

The loss coefficient U_L is evaluated using data from the NOCT test. Those are the measured cell temperature $T_{C,NOCT}$ at an ambient temperature $T_{AMB,NOCT}$ and an irradiance Φ_{NOCT} as listed in Table 2.1. Equation (2.3.5) is rearranged to solve for U_L, neglecting the term $\eta/\tau \, \alpha_{ave}$:

$$U_L = \frac{\Phi_{NOCT}(\tau \, \alpha_{ave})}{T_{C,NOCT} - T_{AMB,NOCT}} \qquad (2.3.7)$$

The NOCT test is usually conducted at a total irradiance of 800 W/m², an ambient temperature of 20°C and a wind velocity of 1m/s, not predominantly parallel to the array. The environmental conditions are often quite different than those test conditions. A higher wind speed for instance causes a higher rate of convective heat transfer and has an effect on U_L. But a difference in U_L has a rather small effect on the evaluated cell temperature. Therefore, U_L is assumed to be constant. Since higher wind speed yields a lower cell temperature and hence higher power output, the estimation of the power output is conservative at higher wind speed.

2.4 EFFECT OF IRRADIANCE AND TEMPERATURE ON I-V BEHAVIOR

The response of a PV cell to different illumination levels is shown in Figure 2.5. The family of I-V curves could correspond to 5 different times of a day, with solar noon represented through an irradiance of 1000 W/m² and early morning or late afternoon represented through an irradiance of 200 W/m². Obviously irradiance has a large effect on short circuit current, i.e. on the horizontal arm of the I-V curve, while the effect on open circuit voltage, i.e. the relatively vertical arm of the curve, is rather weak. Regarding the maximum power output of a PV cell, it is obvious that when the irradiance is higher the cell generates more power.
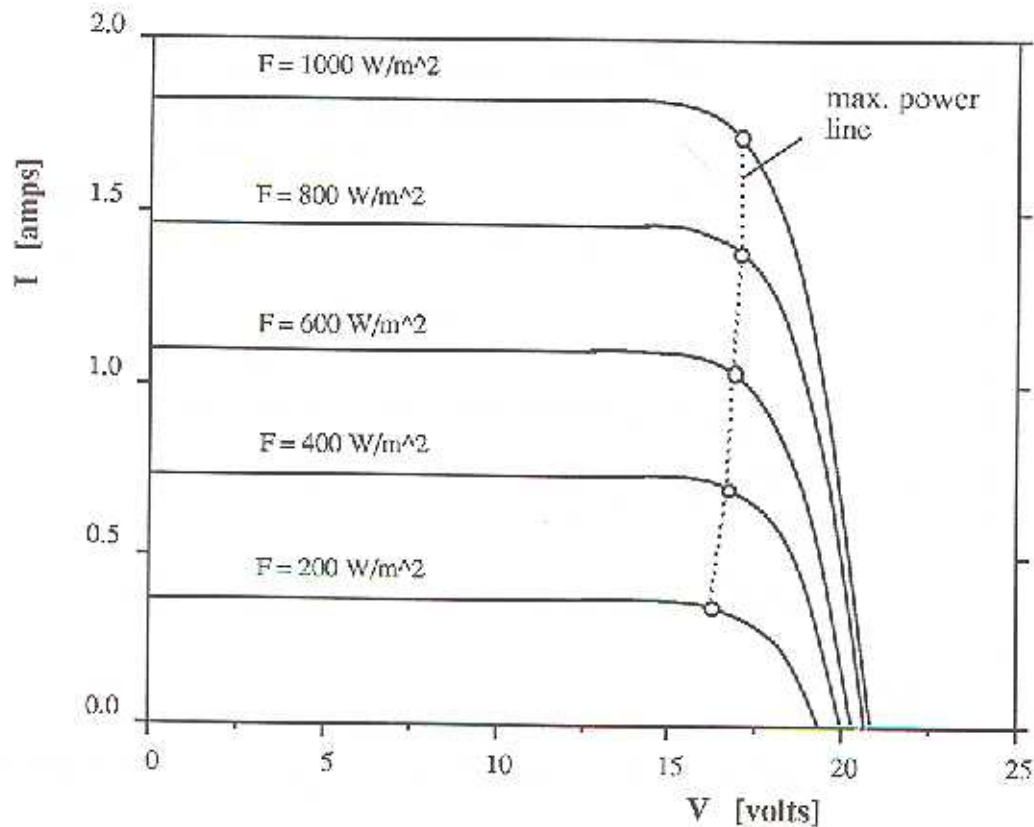
Figure 2.5 Effect of irradiance on I-V characteristics. Solarex MSX-30 module; fixed Tcell = 30°C

As mentioned in the previous chapter, the temperature has an effect on the output of a PV cell. As shown in Figure 2.6, increasing the temperature causes the voltage to drop at high voltages. Operating the cell in this region of the curve leads to a significant power reduction at high temperatures. This is a particularly severe problem, since the cell is often operated at the maximum power point, which is within this region. The effect of temperature on short circuit current is small but increases as the irradiance increases.

$$\frac{\partial P}{\partial V} = V \frac{\partial I}{\partial V} + I = 0 \tag{2.5.2}$$

With the current described by equation (2.1.6), the partial derivative of I with respect to V is

$$\frac{\partial I}{\partial V} = -I_O \exp\left(\frac{v(V+IR_s)}{\gamma}\right) \times \frac{v}{\gamma} \times \left(1 + R_S \frac{\partial I}{\partial V}\right) \tag{2.5.3}$$

An explicit expression for $\partial I/\partial V$ is obtained simply by rearranging the equation. Back substitution of this explicit expression into equation (2.5.2) and using I_{MP} for I and V_{MP} for V gives

$$I_L + I_O - I_O \exp\left(\frac{v(V_{MP}+I_{MP}R_s)}{\gamma}\right) \times \left(1 + \frac{\frac{v\,V_{MP}}{\gamma}}{1 + \frac{v\,R_S\,I_O}{\gamma} \exp\left(\frac{v(V_{MP}+I_{MP}R_s)}{\gamma}\right)}\right) = 0 \tag{2.5.4}$$

To eliminate V_{MP} in equation (2.5.4), the general I-V equation (2.1.6) is used, with I_{MP} substituted for I and V_{MP} substituted for V. Rearranging to solve for V_{MP} gives

$$V_{MP} = \frac{\gamma}{v} \ln\left(\frac{I_L - I_{MP}}{I_O} + 1\right) - I_{MP}\,R_S \tag{2.5.5}$$

An implicit expression for I_{MP} is obtained by substituting equation (2.5.5) into equation (2.5.4):

$$I_{MP} + \frac{(I_{MP} - I_L - I_O)\left[\ln\left(\frac{I_L - I_{MP}}{I_O} + 1\right) - \frac{I_{MP} R_S v}{\gamma}\right]}{1 + (I_L - I_{MP} + I_O)\frac{R_S v}{\gamma}} = 0 \qquad (2.5.6)$$

Newton Raphson method is applied to solve for I_{MP} using an initial guess given by

$$I_{MP,GUESS} = \frac{\Phi}{\Phi_{REF}} NP \left(I_{MP,REF} + \mu_{ISC}(T_C - T_{C,REF})\right) \qquad (2.5.7)$$

Once I_{MP} is found, V_{MP} may be calculated using equation (2.5.5) and thus the current and voltage at the maximum power point is determined for a given irradiance and cell temperature.

2.6   TRNSYS COMPONENT FOR A PV ARRAY

In the previous sections of this chapter, all the necessary equations have been derived. These equations form the basis of a *TRNSYS* component. Every *TRNSYS* component has three different groups of information: a set of parameters, an array of input variables, and an array of output variables.

The information flow diagram for the PV array component is illustrated in Figure 2.7. The component is represented as a box. The four inputs and the ten outputs are listed and the arrows pointing in the direction of this information flow, as it is seen from the component, is shown.
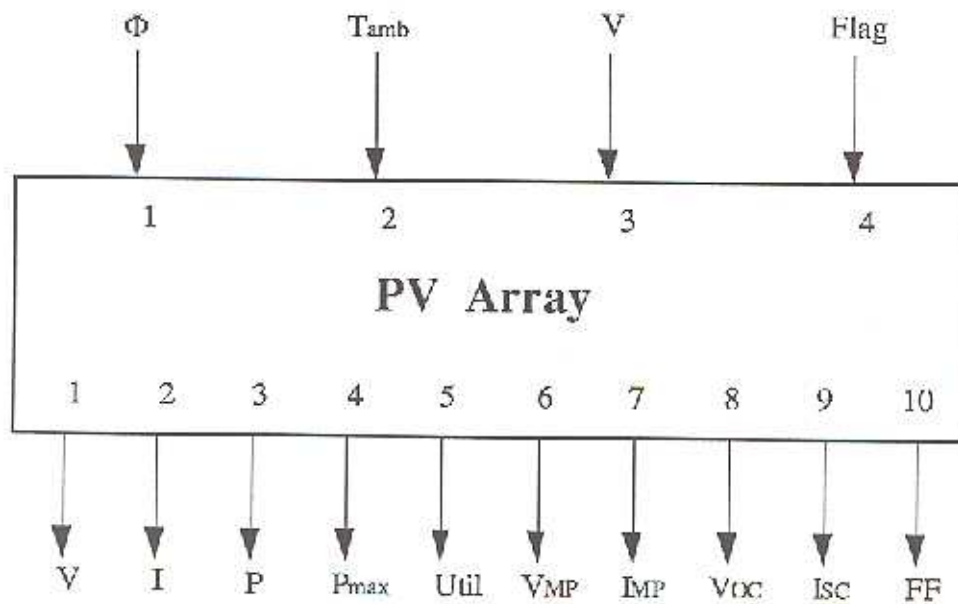
Figure 2.7 Information flow diagram of the PV array component

The eighteen parameters of the component are:

|						
1.)	$I_{SC,REF}$	[amps]		10.)	NS	
2.)	$V_{OC,REF}$	[V]		11.)	NP	
3.)	$T_{C,REF}$	[°K]		12.)	$T_{C,NOCT}$	[°K]
4.)	Ψ_{REF}	[W/m²]		13.)	$T_{A,NOCT}$	[°K]
5.)	$V_{MP,REF}$	[V]		14.)	Φ_{NOCT}	[W/m²]
6.)	$I_{MP,REF}$	[amps]		15.)	AREA	[m²]
7.)	μ_{ISC}	[amps/K]		16.)	$\tau\,\alpha_{ave}$	
8.)	μ_{VOC}	[V/K]		17.)	ε_G	[eV]
9.)	NCS			18.)	R_S	[ohms]

The parameters are characteristic values which are fixed throughout the simulation. The parameter list for the PV array component contains the module specific information such as the measured I-V characteristics at reference condition, NOCT test data and details concerning the array size. Parameter 15) is the module area. If information about $\tau \alpha_{ave}$ is lacking, a good assumption is a value of 0.9. The series resistance can either be provided as a parameter or can be estimated with the method presented in section 2.2.2. If no information about the series resistance is available, parameter 18) is set equal to a negative value and R_s will be evaluated.

Inputs are the time dependent variables such as irradiance (in kJ/m^2) and temperature (in °K), variables which depend on some other function and are subject to the iterative process in finding the proper solution (in this case the voltage) and control variables (Flag).

The need for the first two inputs, irradiance and ambient temperature, is obvious. The choice of using voltage as an input instead of current needs further explanation. At first it would seem to be better to have the current as input, since equation (2.1.6) can then be solved explicitly for voltage. The computational effort involved in calculating the current when the voltage is known could then be avoided. In order to understand why the voltage is the better choice, something has to be said about how *TRNSYS* operates to find a solution.

The goal is to find the operating point of a PV system. In a simple case, a system would be a PV array connected to an electrical load. The electrical behavior of any kind of load can be described, in the same manner as the PV cell, by its I-V characteristic. The operating point is simply given by the intersection of the two I-V curves. In the

case of an ohmic resistance the I-V curve is a straight line through the origin in the I-V plane with the slope 1/R as shown in Figure 2.8 for three different resistances (R1 < R2 < R3).
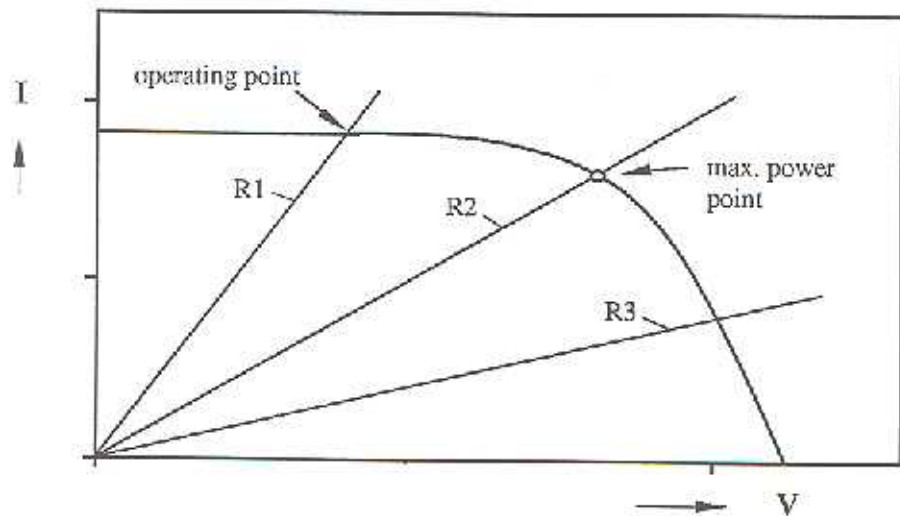

Figure 2.8 PV generator and resistive load I-V characteristics. Operating points and the maximum power point locus is shown.

The resistance R2 is the optimal resistance, because its I-V curve intersects exactly at the cell's maximum power point. Analytically the operating point could be found by solving the system of two equations describing the PV array and load I-V curve. In the *TRNSYS* approach the information which is necessary to solve the system of equations is distributed into the different components. In other words the equation describing the I-V behavior of the PV array is included in the PV array *TRNSYS* component, and the equations describing the load I-V characteristics are included in the *TRNSYS* load components. Hence the operating point cannot be found as proposed above.

The operating point has to be found by an iterative process of exchanging

information between the different components. A recyclic information loop can be generated when the two components are connected as illustrated in Figure 2.9.
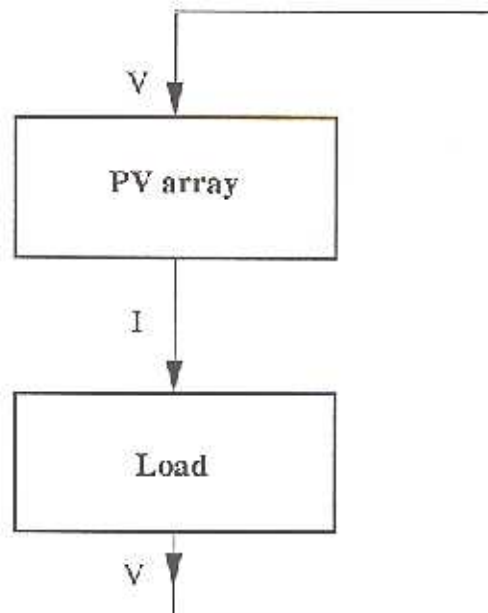
Figure 2.9 Recyclic information flow between the PV array and the load

In a real system the physical quantities flowing through the wires would be the current and in a certain sense, the voltage too. In the same manner voltage and current are chosen as the information to be transferred between the components. The iteration process begins with an initial guess, V, as an input to the PV array component. The PV array component calculates the corresponding current being shifted to the load component. The load component produces a new voltage serving as a second guess for the PV array component. This process of successive substitution is continued until convergence is obtained, and the operating point is found. For a better understanding, the procedure is visualized in the I-V graph in Figure 2.10. Since the environmental